Bollettino di Geofisica Teorica ed Applicata Vol. 61, n. 2, pp. 159-176; June 2020
DOI 10.4430/bgta0302

A knowledge-guided fuzzy inference approach for integrating geophysics, geochemistry, and geology data in a deposit-scale porphyry copper targeting, Saveh, Iran

S. Barak, M. Abedi and A. Bahroudi

School of Mining Engineering, University of Tehran, Iran

(Received: 14 April 2019; accepted: 12 October 2019)

ABSTRACT The main aim of this study is to investigate the applicability of a Fuzzy Inference System (FIS) approach to produce a copper mineral potential map (MPM) at the Saveh area in the Markazi province of Iran. Seven indicator layers extracted from the geological, geochemical, and geophysical data sets are casted in a geospatial database for data integration. Indicator layers are rock types, alterations, Cu concentration anomaly, main geochemical principal component anomaly, reduced-to-pole magnetic data, electrical chargeability, and electrical resistivity. A fuzzy gamma operator is used at the first phase of exploratory data integration to produce three criterium layers that are geology, geochemistry, and geophysics. Then, at the second phase, the FIS is implemented in three main stages consisting of: 1) fuzzification of input/output data, 2) designing an inference engine, and 3) defuzzification of integrated data. The mineral favourability map is prepared and reclassified into five zones through a multifractal approach at the third phase. In order to evaluate the accuracy of the FIS method, the productivity index of 18 boreholes are utilised to examine the correlation between the mineralised zones and the MPM output. Whereby the synthesised indicator layers demonstrated a Pearson's linear correlation coefficient of 0.44 in recognising copper mineralisation at depth. In addition, the eastern and central portions of the Saveh prospect were proposed as favourable potential zones for further mining operation.

Key words: fuzzy inference system, mineral potential mapping, Cu mineralisation, Saveh.

1. Introduction

The ultimate goal of a mineral exploration program is to detect new economical depositions in a sought region. Collecting simultaneously various geospatial data sets (e.g. geology, geophysics, and geochemistry), processing these data to extract exploratory indicator layers and data integration are called mineral potential mapping (MPM). Indeed, MPM is a multiple criterion decision-making (MCDM) task which provides a predictive model for categorising of sought areas in terms of ore mineralisation (Abedi and Norouzi, 2012; Abedi *et al*., 2012).

Knowledge and data-driven methods are two major categories developed for MPM to delineate highly favourable areas for exploration of a special sought deposit (Bonham-Carter, 1995; Carranza, 2008). The theory of fuzzy sets and fuzzy logic (Zadeh, 1965) is categorised in the knowledge-driven approach of MPM by which the weight assignment of indicator layers are on

the basis of the decision makers (DMs)' judgments (e.g. D'Ercole *et al*., 2000; Knox-Robinson, 2000; Carranza and Hale, 2001; Porwal *et al*., 2003; Tangestani and Moore, 2003; Abedi *et al*., 2012; Barak et al., 2018a, 2018b). There are various types of fuzzy algebraic operators, that are fuzzy AND, fuzzy OR, fuzzy algebraic product, fuzzy algebraic sum, and fuzzy gamma operator (Mizumoto and Tanaka, 1981). However, among fuzzy algebraic operators, which have been extensively discussed by Zadeh (1965) and Lee (2007), the fuzzy gamma operator is defined as a combinatory operator of both the fuzzy algebraic product and the fuzzy algebraic sum. The contribution of each of these operators is controlled by a gamma parameter that varies at an interval from 0 to 1. Thus, the fuzzy gamma operator allows for more flexible combinations of weighted indicator maps, and could be readily implemented.

Utilisation of fuzzy logic for MPM is not a new idea. After its implementation for the first time in synthesising exploratory indictor layers by An *et al*. (1991), numerous researchers studies have dedicated to investigate the performance of the fuzzy logic for delineation of various types of ore deposits (e.g. Nykänen *et al*., 2008; Joly *et al*., 2012; Lisitsin *et al*., 2013; Lindsay *et al*., 2014). As expressed by Mamdani and Assilian (1975), the inferencing techniques of a FIS are divided into three types that are Mamdani-style, Sugeno-style, and Tsukamoto-style. They are run in three main stages: 1) fuzzification of input/output data, 2) designing a fuzzy inference system, and 3) defuzzification of the output (Mamdani and Assilian, 1975; Sabri *et al*., 2013). Among all, the FIS of Mamdani and Tagaki-Sugeno algorithms have been extensively employed in various fields of geoscience (Nguyen and Ashworth, 1985; Gokay, 1998; Acaroglu *et al*., 2008), particularly for mineral exploration (e.g. Alaei Moghadam *et al*., 2015; Porwal *et al*., 2015; Barak *et al*., 2018a, 2018b).

This study focuses on the integration of a multidisciplinary geospatial database comprising of several indicator layers extracted from geology, geophysics, and geochemistry data, pertaining to a deposit-scale porphyry copper zone (i.e. the North Narbaghi) at Saveh district in Markazi province of Iran. A FIS methodology is run in three phases to synthesise indicator layers into a porphyry copper mineral favourability map. At first phase, a fuzzy gamma operator is utilised to prepare three main criteria of geology, geophysics, and geochemistry through integration of their sublayer indicators. Then, in the second phase, a FIS is implemented to integrate these criteria into a single mineral potential map. Finally, a multifractal approach is employed in the third phase to classify the MPM into some favourability zones, whereby the most productive one(s) is suggested for exploratory drillings.

The remainder of this work has been prepared as follows. Second section describes concisely the FIS methodology. Geological setting of the studied area is presented in the third section. In section four, the geospatial data sets are explained for geology, geochemistry, and geophysics in order. Fifth section illustrates how to implement data integration in details. The accuracy of the final synthesised indicator layers for porphyry copper targeting is evaluated and discussed in section six. Finally, the main achievements of this study are concluded in the last section.

2. Methodology

Literatures survey illustrates that the comprehensive explanations and more details of the FISs were studied by many researchers (Monjezi *et al*., 2009; Rezaei *et al*., 2014; 2015). As stated by Tang (2004), Alaei Moghadam *et al*. (2015), and Barak *et al*. (2018a), a FIS is a mapping

technique by which the fuzzy logic conducts the inputs to produce outputs. The FIS recognised as a knowledge-driven MPM method is an artificial intelligence system, which is transparent, intuitive and easy to build (Porwal *et al*., 2015). As declared by Bárdossy and Fodor (2003), the fuzzy set technique is an appropriate method for geoscience applications, because of adoptability, intelligibility and simplicity aspects. Various researchers have employed successfully the FIS in geospatial data analysis to explore mineral depositions (e.g. Alaei Moghadam *et al*., 2015; Porwal *et al*., 2015; Barak *et al*., 2018a, 2018b).

As mentioned, to run a popular inference system, that is a Mamdani-style, three steps of the fuzzification, the inference engine designing, and the defuzzification are required (Mamdani and Assilian, 1975). These steps for MPM are as follows:

(i) fuzzification of input indicator layers. This stage includes assigning fuzzy membership values to the input predictor maps through a fuzzy membership function. There are various types of functions to fuzzify inputs such as triangular, trapezoidal, Gaussian, and so on (Osna *et al*., 2014; Porwal *et al*., 2015; Shams *et al*., 2015; Barak *et al*., 2018a). As discussed by Masters (1993), the selection of a fuzzy membership function is an indispensable stage which can substantially affect the output directly. Among all functions commonly utilised in geoscience applications, triangular, trapezoidal, and Gaussian are popular (Osna *et al*., 2014; Shams *et al*., 2015). For more details, the work by Luo and Dimitrakopoulos (2003) are suggested. Fuzzy membership weights are assigned through the DMs' attitudes towards MPM, but some researchers have employed objective mathematical functions for such task (e.g., Luo and Dimitrakopoulos, 2003; Porwal *et al*., 2003);

(ii) integration of indicator layers or designing an inference engine. This stage for the sake of defining the if-then rules is the most influential section of the technique. Here, the DMs should capture all realistically possible conditions between input indicator layers and final potential map. The number of fuzzy if-then rules in a FIS increases with the increasing of input variables (indicator layers), known as the disadvantage of a FIS technique. Thus, it can be a too complicated model for MPM. To tackle such a deficiency, Alaei Moghadam *et al*. (2015), Porwal *et al*. (2015), and Barak *et al*. (2018a) have proposed the implementation of the whole fusion in two stages, where indicator layers are integrated into three main criteria of geology, geochemistry, and geophysics at the first stage, and, then, these criteria are integrated via a FIS in the second stage;

(iii) defuzzification of output layer. The fuzzified output layer must be converted into a crispy format. Various models have been proposed for defuzzification that are centre of gravity, weighted average, maximum mid centre, and centre of the greatest levels (Klir and Yuan, 1995).

3. Geological setting of the North Narbaghi

A north dipping subduction of the Neo-Tethys Ocean has affected the Iranian plateau begun in the Mesozoic era (Stöcklin, 1968; Berberian and Berberian, 1981). After maturing the subduction zone and the overlying continental magmatic arc, intense igneous activities led to a wide belt consisting of Cenozoic plutonic and volcanic units, which is known as the Urumieh-Dokhtar magmatic assemblage zone (UDMA) in the Iran structural geology map. Such subduction generated

the UDMA as a distinct, linear intrusive-extrusive complex with elongation from the NW to SE of Iran, located among the magmatic-metamorphic Sanandaj-Sirjan zone (SSZ) and the central Iran domain (Nouri *et al*., 2018; Imamalipour and Barak, 2019). The Saveh prospect zone is located at the UDMA zone (Fig. 1), where the UDMA (also known as the Sahand-Bazman or Tabriz-Bazman zones) is the main host of the porphyry and epithermal metallic deposits such as Cu, Au, and Mo (Berberian and King, 1981; Rezaei *et al*., 2015). This ore-bearing zone defined as a ~ 50-100-km wide belt dominated by an Andean-type magmatic arc created at the crust of the Central Iranian Micro-Continent (CIMC) structural unit. The UDMA is discerned by the Cenozoic extrusive and intrusive units with an age of Eocene-Quaternary along with the associated volcanoclastic rocks. Intrusive magmatic units in the UDMA are often the subvolcanic porphyritic granitoid units of diorite, granite, granodiorite, and tonalite rocks (Shahabpour, 2005; Kazemi *et al*., 2018). Igneous activities have frequently occurred in Paleogene, where these volcanic rocks in the Saveh area are thicker than 4 km, and include pyroclastic sequences, lava flows, tuff, and ignimbrites (Stöcklin, 1968; Berberian and Berberian, 1981; Alavi, 2007).

From a detailed geological point of view, the mineralised zone in the North Narbaghi copper deposit indicates a volcano-genetic type of mineralisation, and it is located on the volcanic belt of the UDMA zone. The main rock units dominating the studied area are as follows (Fig. 1):

1) monzogranite to quartz monzonite units as the main host rocks of the Cu mineralisation which were severely dominated by argillic alteration. The number of intrusive rocks in the Saveh region is relatively high, but most of them are exposed as small masses. The age of these masses is attributed to the early Oligocene. The extension of these intrusive masses has been in association with the great lineaments of the region. In fact, all of intrusive masses around the Saveh were observed on the margins and sides of the fractures. Therefore, it can be assumed that the intrusive masses of this region were fed by a batholith source. Two types of alteration were observed in this unit that are phyllic and argillic alterations. The phyllic alteration was seen in portions with minerals including pyrite, sericite, and quartz, and the areas with depleted Cu mineralisation were the masses severely affected by the argillic alteration. In some parts, the intrusive masses were unaltered;
2) basaltic andesite unit with silicic alteration. Volcanic activity in the area gave rise to the formation of the basaltic andesite within the porphyritic hornblende andesite unit, which has a dark gray color, with a distinct outcrop than the surrounding rocks. These rocks are mostly surrounded by the monzogranite and quartz monzodiorite units;
3) porphyritic hornblende andesite types with propylitic alteration. The influence of the severe alteration of the coarse crystals, such as chlorite, epidote, and carbonate, emerges clearly in the andesite, which has led to the transformation of plagioclase and amphibole into these minerals. The andesite unit with an Eocene age is the oldest and the widest rock unit in the south of the mineralised region. Chlorite alteration was sporadically obvious and intensively increased in proximity to the mineralised areas (Ghalamghash, 1998; Ramazi and Jalali, 2015).

Fault lineaments with little outcrop in the area did not have much effect on the Cu mineralisation. With association to the disseminated type of the Cu mineralisation, the effect of the faults just led to locally trivial Cu enrichment. The largest fault observed in the region was with an approximate N-S trend in the west of the area (Dehghan Nayeri, 2018).

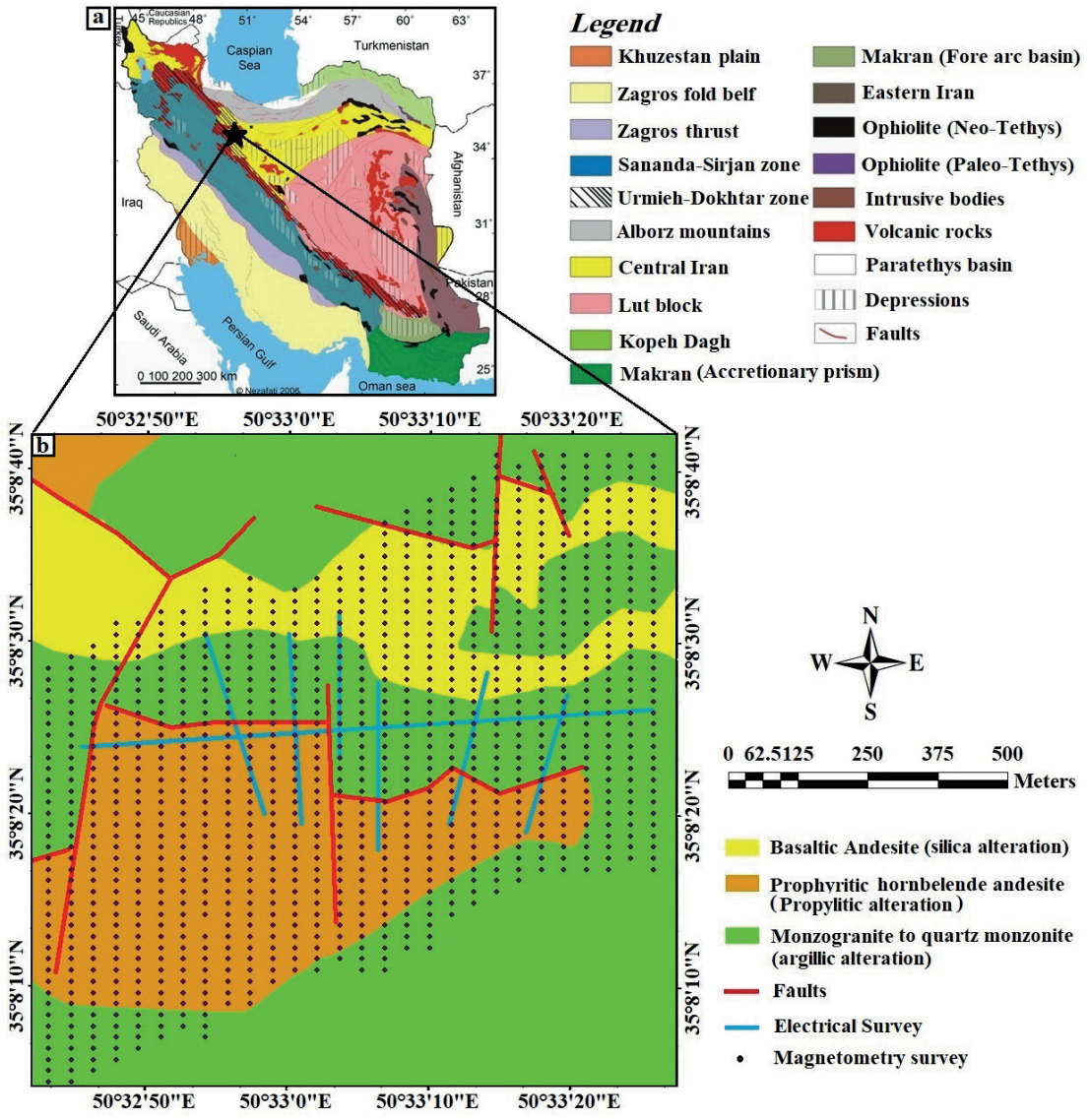

Fig. 1 - The general structural geological map of Iran (a), and the simplified geological units in the North Narbaghi copper deposit (b).

4. Geospatial data sets

Taking the conceptual model of porphyry copper mineralisation into account (Sillitoe, 2010), seven indicator layers were derived from the geological, geochemical, and geophysical data sets. These layers are explained in this section to construct a geospatial database. Each indicator layer was scored at an interval of [0, 1] by a group of DMs with expertise in porphyry copper exploration to suppress scaling effects perturbing the integration result. Each indicator layer was discretised into pixel sizes of 40×40 m^2 to construct the multidisciplinary database. After generation of all indicator layers, in the first phase of MPM, three criteria layers of geology, geochemistry, and geophysics are constructed through a fuzzy gamma operator.

4.1. Geological indicators

Due to conceptual model of Cu mineralisation (Arribas 1995; Singer *et al*., 2002; Sillitoe, 2010) and geoscientist DMs' attitudes towards MPM, monzogranite to quartz monzonite units were gained the highest score as the main host rocks of the copper depositions (Fig. 2a). In addition, the disseminated nature of the Cu mineralisation with the phyllic alteration scattered in these units were assumed the highest scores in the alteration layer (Fig. 2b). Subsequently, the porphyritic hornblende andesite and the basaltic andesite units were assigned lower scores, respectively. The lowest score was also assigned to the propylitic alteration which has surrounded the main zones of mineralisation. Since there were not any evidence of the Cu mineralisation in association with the fault activities in the North Narbaghi, they were not taken into consideration as an individual indicator layer. Then, the geology criterion of the Saveh area was prepared

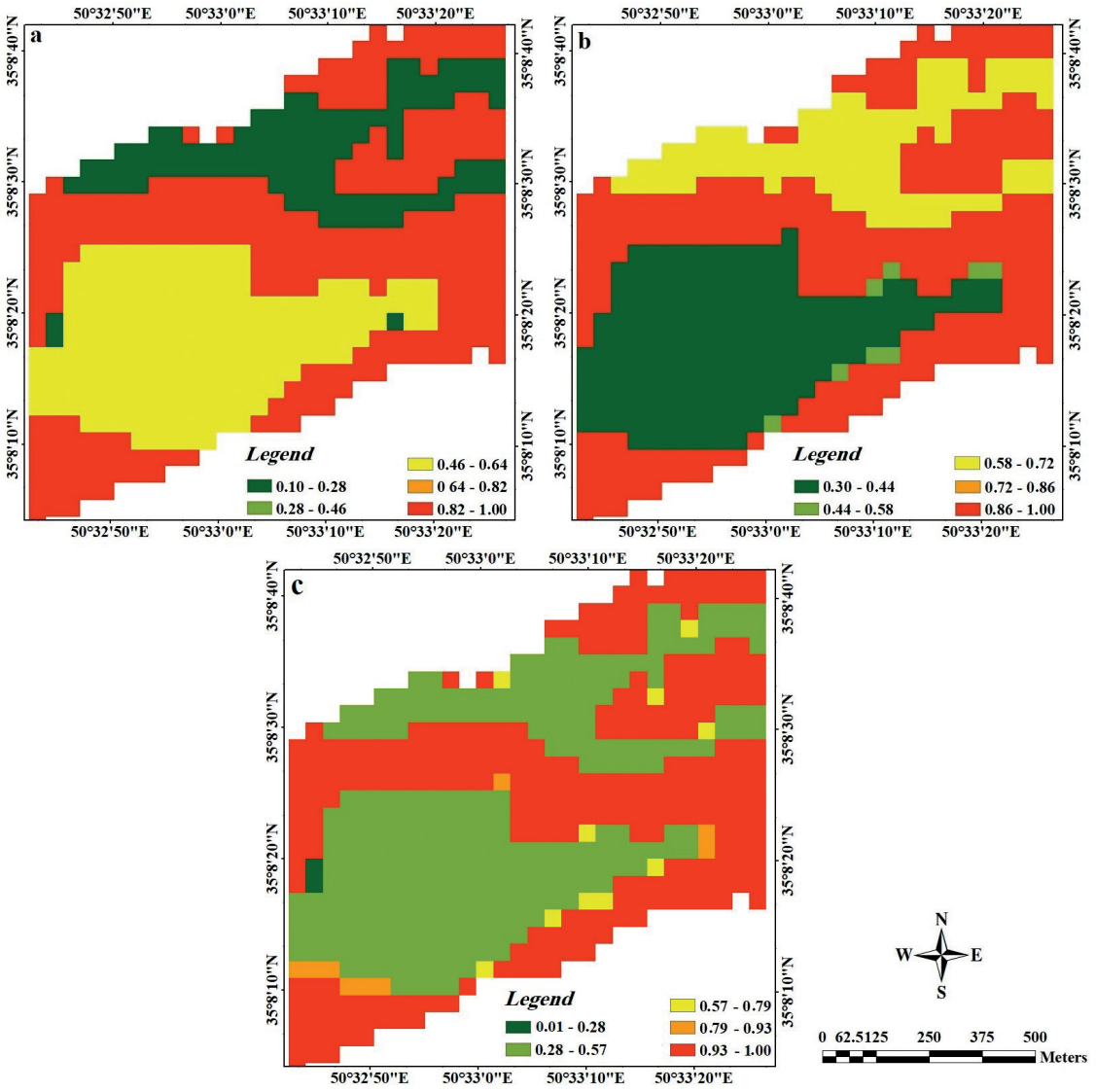

Fig. 2 - The geological indicator layers: a) rock type; b) alteration; c) geological criterion.

through the integration of rock types and alterations using a fuzzy gamma operator. The gamma value is determined by a trial-and-error test which was equivalent to 0.9 (Fig. 2c). Integration of geological indicators into a single geology criterion (first phase) can facilitate the design of if-then rules when running a FIS.

4.2. Geochemical indicators

Lithogeochemical survey was conducted in the area, where 47 samples were collected systematically. The distance of the sampling was less over the monzogranite and quartz monzonite units, where evidences of the Cu mineralisation were manifested. The descriptive statistical characteristics of the main elements, correlated strongly with the Cu element, has been presented in Table 1. Pearson's linear correlation coefficients for six elements are tabulated in Table 2, and they indicate the enrichment of Mo, Zn, Co, As, Sb, and Li versus the Cu concentration. This correlation was negative for Mg (-0.567), where there was depletion of the Mg element over the mineralised zones. The non-normal distribution of the Cu concentration was evident based on the histogram, box, and quantile-quantile (q-q) plots shown in Figs. 3a, 3b, and 3c, respectively. Such a strong non-normal distribution can be relevant to favourable zones of copper mineralisation, where the background copper concentration with a mean value of 2256 ppm has enriched to an amount of 13,333 ppm. Fig. 4a indicates the geochemical map of the Cu concentration in the area where two distinct zones were visible as the geochemically anomalous zones.

The principal component analysis (PCA) as a well-known multivariate statistical technique and a

Table 1 - Descriptive statistical summaries of main correlated elements (in ppm).

Element	Min	Max	Mean	Median	Std.	Skewness	Kurtosis
Cu	3.83	13333.00	2256.10	134.13	4333.30	1.880	4.95
Mo	0.66	11.30	3.12	1.94	3.30	1.510	3.99
Zn	7.53	568.00	69.17	24.00	103.98	2.790	12.50
Co	6.00	167.00	45.44	20.57	53.92	1.480	3.64
As	3.33	5960.00	668.46	42.00	1483.1	2.500	v8.11
Sb	3.33	229.00	27.33	5.51	55.82	2.640	8.66
Mg	0.06	3.07	1.06	1.06	0.78	0.690	3.06
Li	0.75	144.00	22.13	10.00	32.56	2.078	6.76

Table 2 - Pearson's linear correlation coefficient.

Element	Cu	Mo	Zn	Co	As	Sb	Mg	Li
Cu	1.000							
Mo	0.845	1.000						
Zn	0.573	0.440	1.000					
Co	0.872	0.734	0.504	1.000				
As	0.869	0.863	0.518	0.748	1.000			
Sb	0.816	0.869	0.464	0.653	0.748	1.000		
Mg	-0.567	-0.563	-0.292	-0.605	0.653	-0.478	1.000	
Li	0.631	0.444	0.388	0.811	-0.605	0.389	-0.543	1.000

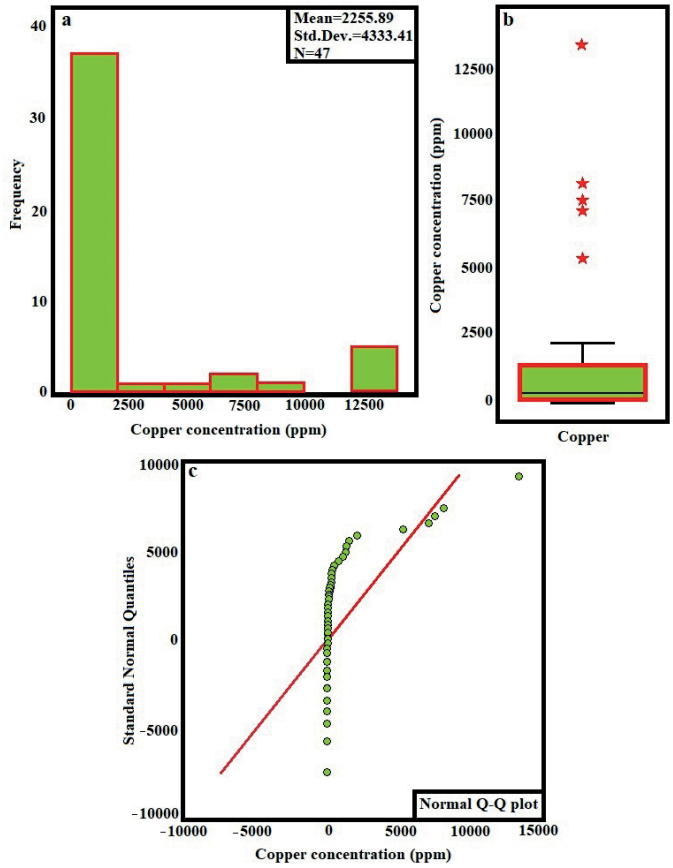

Fig. 3 - The statistical charts from the lithogeochemical samples in the prospect region: a) histogram; b) box; c) Q-Q plots of the Cu concentration.

dimension-reduction tool was employed to the eight lithogeochemical elements. This technique leads to a main principal component (PC) indicator layer in strong association with the Cu mineralisation. In this analysis, the PC scores are calculated by the projection of the original geochemical data onto the PC axes (eigenvectors). The elements of the eigenvector that compute the PC scores of the original input data are named loadings (or eigenvalues), which indeed are coefficients of a linear equation for introducing an eigenvector. The original PCs usually are rotated to maximise the elements' loading in contrast. Simply speaking, the process involves moving each PC axis to a new position so that projections from each variable onto the PC axes are either near the extremities or near the origin. Therefore, high loadings attain +/–1 values and low ones tend to 0 (Davis, 2002; Abedi *et al*., 2013). Table 3 has tabulated the eight PC components, where PC1 with about 68.5% of variation variance has the most close consistency with the Cu mineralisation. Fig. 4b plotted the PC1 indicator map, while two mineralised zones were distinguished from the PCA analysis result of the main correlated elements pertaining to the Cu mineralisation. Finally, the geochemical indicator criterion of the Saveh area was generated through the integration of the Cu concentration anomaly and the PC1 indicator map, assuming a fuzzy gamma operator ($\gamma = 0.95$, Fig. 4c).

4.3. Geophysical indicators

Magnetometry and geo-electrical surveys, as two prevalent geophysical tools, can approve valuable pieces of information about the types of alteration, rock, and ore mineralization,

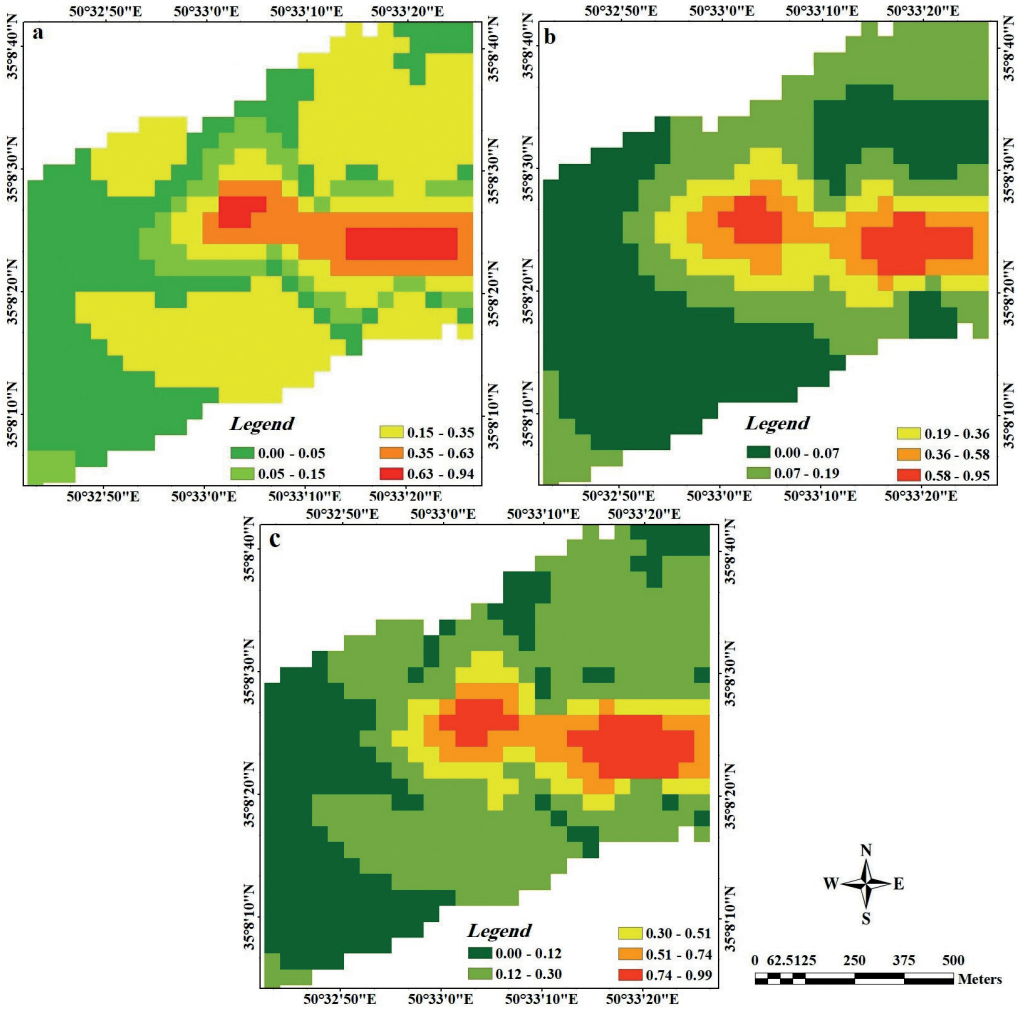

Fig. 4 - The normalised geochemical indicator layers: a) Cu concentration; b) main principle component; c) geochemical criterion.

Table 3 - The PC analysis for correlated lithogeochemical elements, where the PC1 was chosen as the main factor in association with the Cu mineralisation.

	PC1	PC2	PC3	PC4	PC5	PC6	PC7	PC8
Mo	0.381	-0.284	-0.211	-0.024	-0.434	0.725	-0.113	0.047
Cu	0.405	-0.052	0.038	0.134	-0.381	-0.537	-0.614	-0.059
Zn	0.262	-0.055	0.869	-0.400	0.026	0.104	0.039	-0.016
Co	0.386	0.294	0.030	0.268	-0.395	-0.197	0.705	0.017
As	0.397	-0.281	-0.070	0.125	0.445	-0.107	0.056	0.728
Sb	0.374	-0.438	-0.143	0.039	0.400	-0.097	0.183	-0.666
Mg	-0.291	-0.381	0.408	0.766	-0.077	0.101	-0.006	-0.018
Li	0.303	0.641	0.084	0.378	0.382	0.324	-0.273	-0.139
% variance	68.510	11.390	8.970	6.090	2.560	1.430	0.880	0.170

particularly for porphyry-type deposits (Thoman *et al*., 1998; Clark, 1999; John *et al*., 2010). The porphyry Cu deposits are often surrounded by contrasting zones of different alterations centred on the main source of mineralisation. Such alteration types are generally localised by fluctuations of the magnetic field intensities over their regions. Weak background magnetic intensity increases over the potassic zone (due to iron-oxide contents such as magnetite), decreases over the sericitic/phyllic zones, and gradually intensifies over the propylitic zone. Similar to the magnetic anomalies, the lowest electrical resistivity (Res) and the highest induced polarisation (IP) anomalies are associated with the sericitic/phyllic alteration that has high sulfide content. Since the potassic alteration as the core of the porphyry-type deposits depletes in total sulfide minerals and the distal zone of the propylitic alteration has low amounts of pyrite mineral, they are frequently corresponded to the regions with higher resistivity and lower polarisation anomalies.

Magnetometry survey was carried out along 28 N-S profiles with 40 m spacing for acquisition of 1077 data samples at station interval of 20 m. The Earth's magnetic field intensity was about 47,680 nT with an inclination and declination angles of 53.5° and 4.3°, respectively. Firstly, the total magnetic anomalies over the prospect region was obtained with a distinct anomalous region at the southern part of the area over the porphyritic hornblende andesite unit despite of no evidences of the Cu mineralisation based on the geological field operation. After eliminating the background magnetic field, the reduced-to-pole (RTP) transformation of the residual magnetic data was conducted to eliminate the inclination influence of the induced magnetic field by putting it at the north pole. In fact, it corrects the location of the magnetic anomaly by moving the positive portion of the observed signal over the causative source, amplifies the observed magnetic signal, and generates almost a symmetric positive anomaly. The RTP indicator layer, shown in Fig. 5a**,** depicted that the background magnetic anomalies have decreased at the centre of the Narbaghi, where it was mostly in association with the monzogranite to quartz monzonite units with intense phyllic alteration.

To investigate the electrical properties of the subsurface layers at the region, seven time-domain direct current electrical resistivity tomography (ERT) profiles, with electrode spacing of 20 and mostly 40 m, have been surveyed to image the resistivity and induced polarisation variations at depth. The measurements were applied by two configurations of pole-dipole and pole-pole arrays to obtain data from deeper sources. Since the aim of this study was to generate 2D MPM maps, two horizontal slices from the inverted electrical models were extracted. These depth slices were chosen at the centre of probable Cu mineralisation zone. Figs 5b and 5c revealed the normalised values of the IP and Res maps used in designing of the geospatial database. Both maps showed that the central part of the prospect area had more favourability for the Cu mineralisation, where the phyllic alteration scattered among the monzogranite to quartz monzonite units. Finally, the geophysical criterion at the Saveh area was prepared through the integration of the RTP, IP and Res indicators, using a fuzzy gamma operator ($\gamma = 0.88$, Fig. 5d).

5. Mineral potential mapping

A new Mamdani FIS method is employed here to generate the MPM. In order to determine the existence of Cu mineralisation, three main criteria of geology, geochemistry, and geophysics were prepared as input parameters in the first phase. In the second phase, the FIS is used to generate an

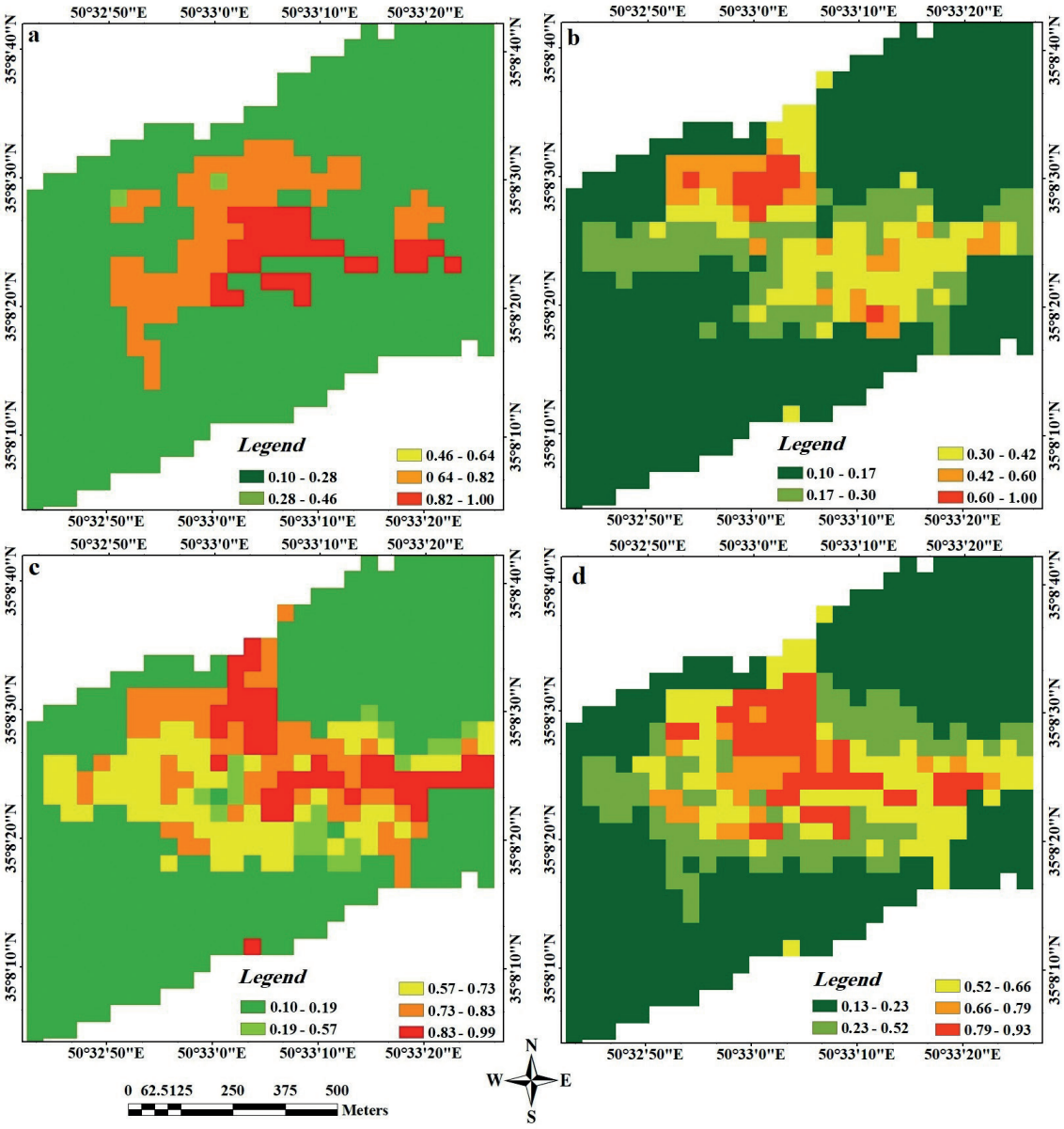

Fig. 5 - The normalised indicator layers of the RTP magnetic data (a), electrical chargeability (IP) (b), electrical resistivity (Res) (c), and geophysical criterion (d).

integrated map. Fig. 6 indicates the decision tree flowchart of these two phases for MPM. To run the FIS in the second phase, the following steps are considered:

i) fuzzification: the first step of the FIS integration approach is a mathematical procedure that converts numerical variables to language variables for both input and output data. It is normally implemented by fuzzy membership functions. Literature review indicates that the triangular and trapezoidal membership functions are used in the most studies. Nevertheless, the trial and error method is used to achieve the optimum membership functions in the current study. Here, the trapezoidal membership functions were used for

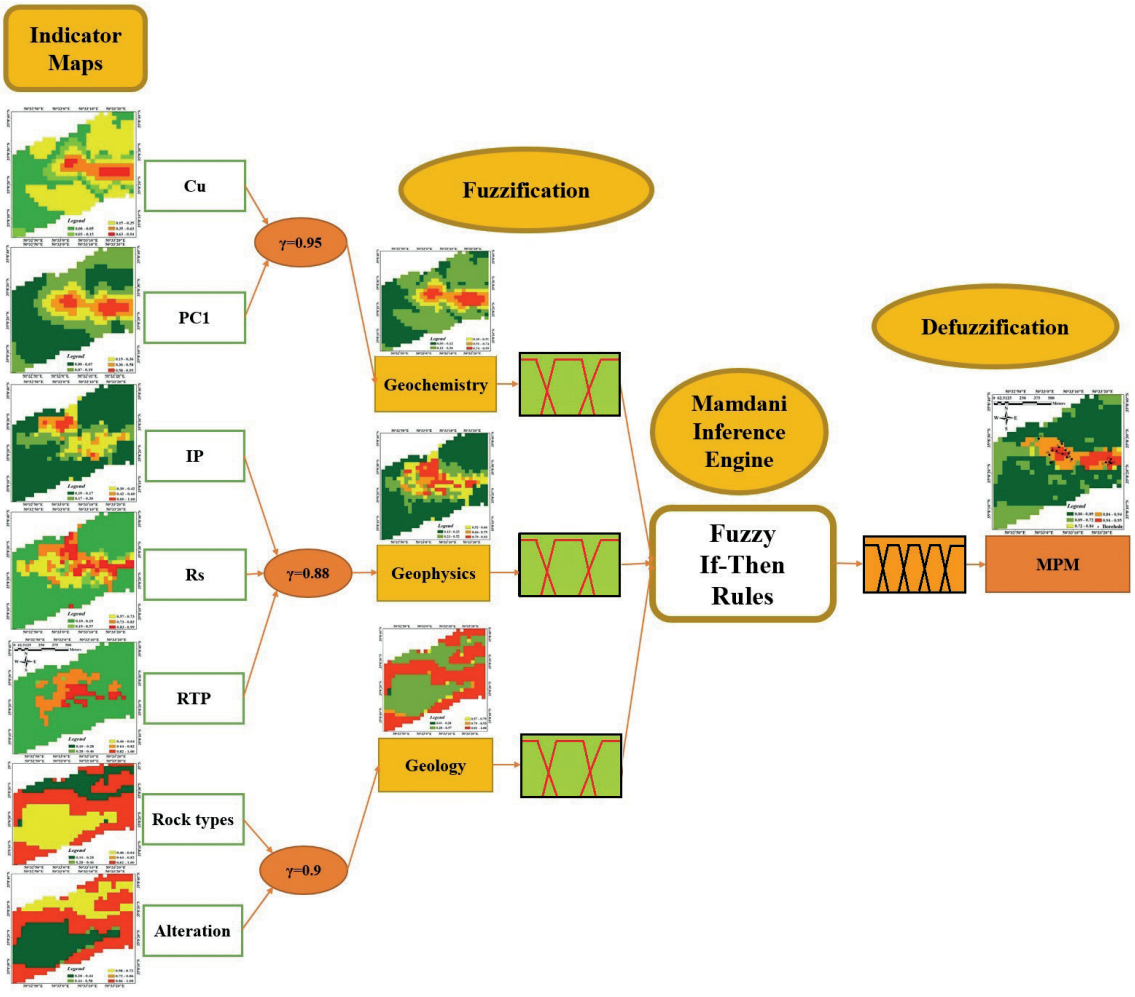

Fig. 6 - Decision tree flowchart for generating final potential map.

fuzzifying geological, geochemical, and geophysical criteria. For input criterion, three linguistic variables were defined including "poor", "average" and "strong" potential (Figs. 7a, 7b, 7c), while for output layer (MPM) five linguistic variable have been used, that are "poor", "below average", "average", "above average" and "strong" potential (Fig. 7d);

ii) inferencing engine: in this step sufficient fuzzy "if-then" rules are designed to create a powerful "rule base" in order to indicate the relations between the input and output variables. These rules were applied based on the expert DMs. As aforementioned, to deal with increasing numbers of the if-then rules, the integration approach of this study was performed in two phases. Firstly, the indicator layers were integrated by gamma operators and subsequently three main criteria were prepared. Secondly, the FIS approach is used to integrate the main criteria (Fig. 6). Some of the defined rules have been tabulated in Table 4 and the simplified procedure of integration has been depicted in the Fig. 8;

iii) defuzzification: as mentioned by Porwal *et al*. (2015), the centroid of area is the most widely used model for defuzzification, which can be formulated as follows:

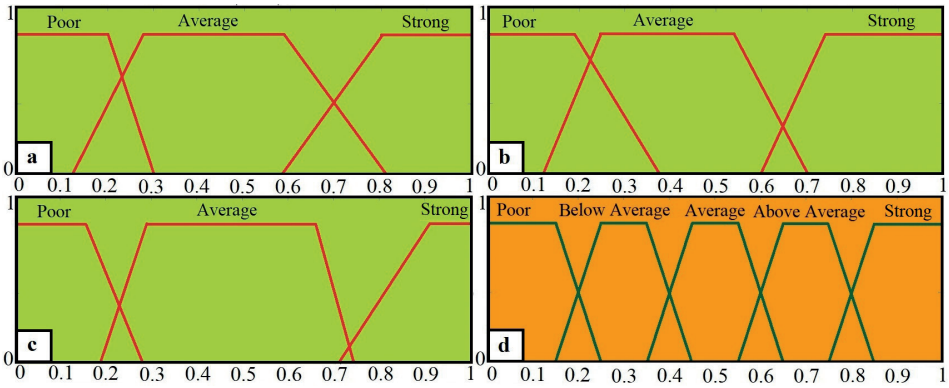

Fig. 7 - Membership functions taken into account for: a) geological criterion; b) geochemical criterion; c) geophysics criterion; d) output mineral potential map.

$$z^* = \frac{\int \mu_{\bar{A}}(x) x \, dx}{\int \mu_{\bar{A}}(x) dx} \tag{1}$$

where, $\mu_{\bar{A}}(x)$ illustrates the degree of the fuzzy membership for values of x, and finally the term Z^* presents the centre of gravity for the membership function values (Fig. 8). Eventually, crispy output is obtained in this step. For instance, in Fig. 8, if the pixel values of the geological, geochemical, and geophysical criteria are respectively 0.74, 0.61, and 0.20, the integrated pixel value will be 0.35.

Table 4 - Examples of if-then rules in the FIS.

Rule	Geology	Geochemistry	Geophysics	Mineral Potential
1	Poor	Poor	Poor	Poor
2	Poor	Average	Poor	Poor
3	Average	Poor	Average	Average
4	Strong	Strong	Average	Above Average
5	Strong	Strong	Strong	Strong

The concentration-area (C-A) multifractal approach was applied to reclassify the area of generated mineral potential map into some favourability zones, which are consistent with separating anomalous regions from background. Experts have studied several techniques for diagnosing anomalous and promising zones. As presented by Turcotte (1997), the fractal relationship exists among the numerous of ore deposits with moderate concentration of different parts. Cheng *et al.* (1994) firstly proposed the C-A technique for extracting anomalous areas with best results. The model was expressed by the following equation:

$$A(\rho \leq \delta) = K \rho^{-\beta} \tag{2}$$

where $A(\rho)$ is the area with the concentration greater than a value ρ, δ denotes a threshold, β is the fractal dimension, and K is a constant.

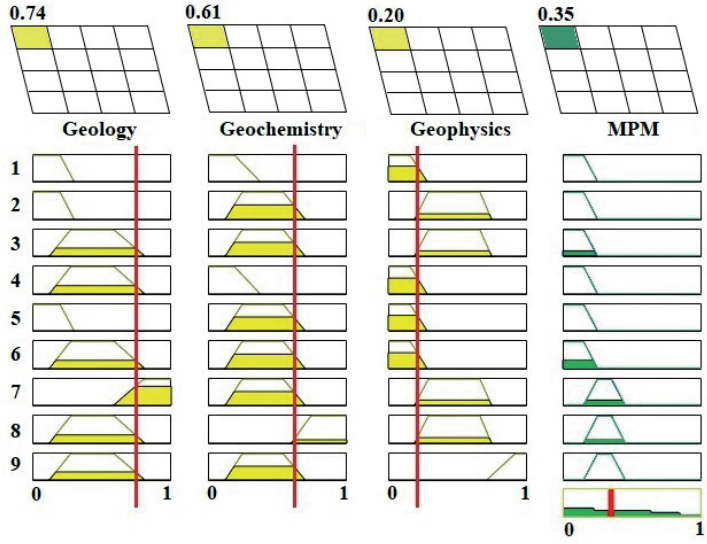

Fig. 8 - The simplified procedure of integrating layers by the FIS method.

In this work for better consequence, the crispy output derived from the defuzzification of the integrated criteria was reclassified into five classes in terms of favourability for copper mineralisation through the C-A fractal-based curve (Fig. 9a), and the MPM of the porphyry copper mineralisation at the North Narbaghi in the Saveh district was prepared (Fig. 9b).

6. Discussion

MPM is a multiple criteria decision task requiring simultaneous consideration of geospatial data sets involving the geological, geochemical, and geophysical indicators. The MPM produces a predictive model for outlining the prospective areas. The efficiency of a FIS method as an artificial intelligence system was examined here to discover porphyry copper mineralisation in the Saveh area. Geospatial database consisted of three main indicator criteria of the geology (surface studies), geophysics (magnetometry and electrical surveys), and geochemistry. A group of DMs in the field of porphyry Cu exploration, with various disciplines in mineral exploration, was gathered together to guide the MPM process. Finally, seven indicator layers were extracted to implement the FIS method in three phases, where a distinct ribbon at the centre of the studied region was manifested as the most favourable zones for exploratory drillings (Fig. 9b). Such promising potential zone located at the monzogranite to quartz monzonite units.

The central portions of the North Narbaghi copper mineralisation were drilled by 18 vertically boreholes to investigate its mining prospectivity. The productivity index of each drilled borehole was calculated in Table 5 to evaluate the efficiency of the MPM. The productivity value was calculated from multiplying Cu concentration (in ppm unit) by its ore thickness (in metre) along each drilled borehole, finally normalised by the total length of borehole. Indeed, the productivity index has presented the average of the copper grade along the borehole. Fig. 9b has indicated borehole locations. The scatter plot of the productivities versus the MPM amounts extracted at the locations of drillings were plotted in Fig. 9c. The Pearson's linear correlation coefficient (ϱ) for the fitted linear curve was also calculated to evaluate the performance of the MPM. It is

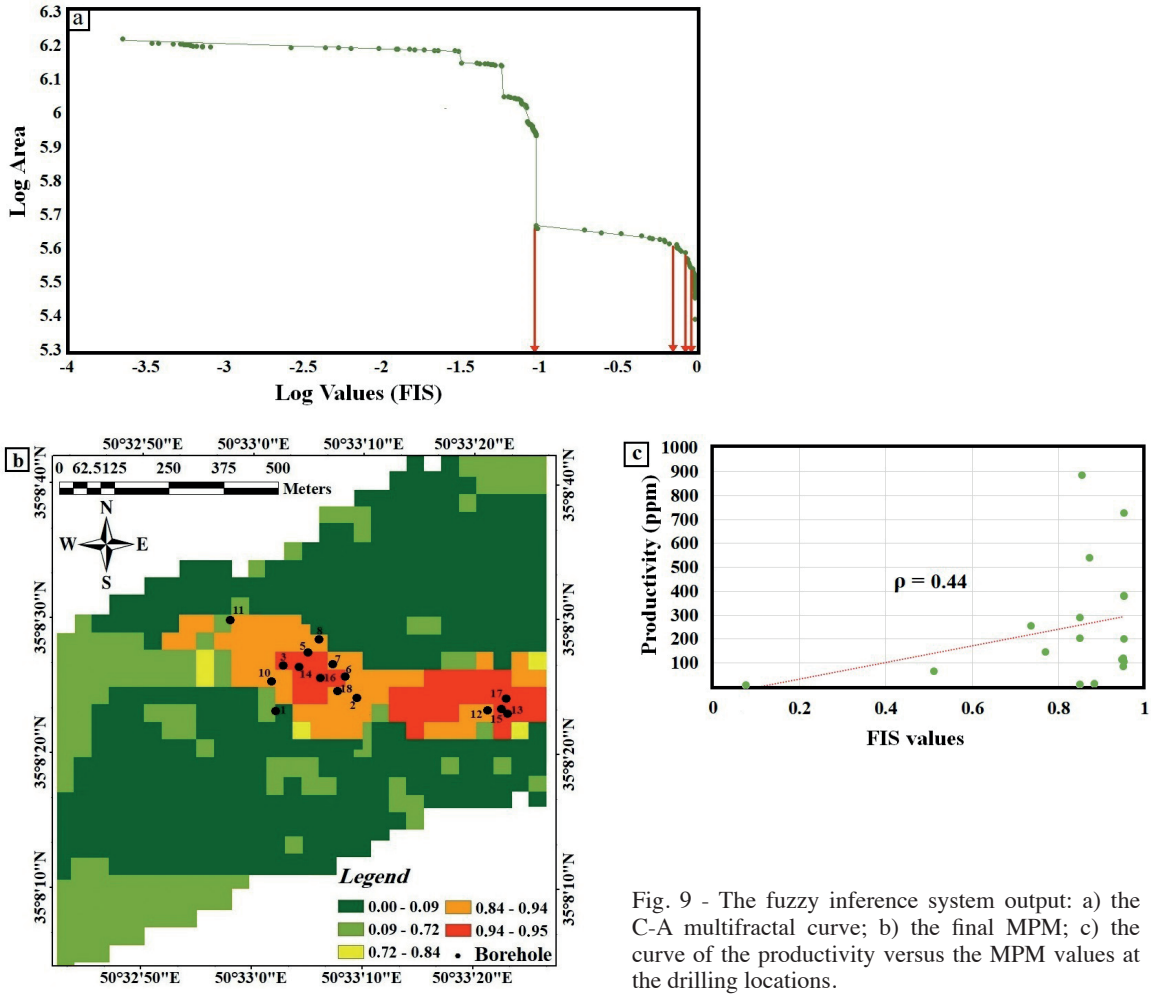

Fig. 9 - The fuzzy inference system output: a) the C-A multifractal curve; b) the final MPM; c) the curve of the productivity versus the MPM values at the drilling locations.

evident that positive correlation must happen when the MPM output is in consistency with the mineralised zones. It attained equal to 0.44.

Since produced MPM in this work was 2D for a deposit-scale prospect zone, the importance of drilled boreholes through calculation of the productivity index were projected and mapped on the surface. Indeed, it facilitated the evaluation of the performance of the MPM by comparison to the drilling results. It should be noted that some indicator layers such as those derived from the geophysical criteria (i.e. RTP, IP, and Res) had information from deep-seated sources. In other words, the effect of blind targets can be manifested on the surface geophysical data. Therefore, 2D MPM could provide valuable information about deep targets in case of involving geophysical indicators.

7. Conclusion

The main aim of this study was to delineate probable porphyry copper mineralisation at the north Narbaghi in the Saveh, Markazi province of Iran. A fuzzy inference system was implemented

Table 5 - The descriptive of the boreholes with their productivity values.

Borehole ID	Length (m)	Productivity (ppm)
1	224.35	8.38
2	184.45	84.62
3	128.70	885.26
4	110.40	199.99
5	179.20	378.85
6	96.10	167.22
7	152.75	726.78
8	55.00	107.38
9	52.00	205.02
10	93.40	14.68
11	96.00	290.52
12	78.00	382.40
13	126.00	696.23
14	56.60	11.02
15	142.00	113.84
16	113.00	119.26
17	71.80	732.55
18	54.00	13.44

in three phases to integrate seven indicator layers derived from geology, geochemistry, and geophysics data. Generated mineral favourability map located a distinct ribbon zone at the centre of the area, where such a potential zone was derived from a concentration-area multifractal analysis. Result of drillings in this zone showed copper occurrences at depth. Note that the 2D copper potential map has an acceptable correlation with the grade productivity of drillings.

Acknowledgements. The authors would like to express their sincere thanks to the School of Mining Engineering, University of Tehran, for all supports. We also acknowledge the financial support of the University of Tehran for this research under grant number of 30646/1/02.

REFERENCES

Abedi M. and Norouzi G.H.; 2012: *Integration of various geophysical data with geological and geochemical data to determine additional drilling for copper exploration*. J. Appl. Geophys., **83**, 35-45.

Abedi M., Norouzi G.H. and Bahroudi A.; 2012: *Support vector machine for multiclassification of mineral prospectivity areas*. Comput. Geosci., **46**, 272-283.

Abedi M., Torabi S.A. and Norouzi G.H.; 2013: *Application of fuzzy AHP method to integrate geophysical data in a prospect scale, a case study: Seridune copper deposit*. Boll. Geof. Teor. Appl., **54**, 145-164.

Acaroglu O., Ozdemir L. and Asbury B.; 2008: *A fuzzy logic model to predict specific energy requirement for TBM performance prediction*. Tunnelling Underground Space Technol., **23**, 600-608.

Alaei Moghadam S., Karimi M. and Sadi Mesgari M.; 2015: *Application of a fuzzy inference system to mapping prospectivity for the Chahfiroozeh copper deposit, Kerman, Iran*. J. Spatial Sci., **60**, 233-255.

Alavi M.; 2007: *Structures of the Zagros fold-thrust belt in Iran*. Am. J. Sci., **307**, 1064-1095.

An P., Moon W.M. and Rencz A.; 1991: *Application of fuzzy set theory to integrated mineral exploration*. Can. J. Explor. Geophys., **27**, 1-11.

Arribas A.J.; 1995: *Contemporaneous formation of adjacent porphyry and epithermal Cu-Au deposits over 300 ka in northern Luzon, Philippines*. Geol., **23**, 337-340.

Barak S., Bahroudi A. and Jozanikohan G.; 2018a: *Exploration of Kahang porphyry copper deposit using advanced integration of geological, remote sensing, geochemical, and magnetics data*. J. Min. Environ., **9**, 19-39.

Barak S., Bahroudi A. and Jozanikohan G.; 2018b: *The use of fuzzy inference system in the integration of copper exploration layers in Neysian*. Iran. J. Min. Eng., **13**, 21-35.

Bárdossy G. and Fodor J.; 2003: *Geological reasoning and the problem of uncertainty*. In: Proc., IAMG 2003, Modeling Geohazards, Portsmouth University, Portsmouth, UK, 5 pp.

Berberian F. and Berberian M.; 1981: *Tectono-plutonic episodes in Iran*. In: Gupta H.K. and Delany F.M. (eds), Zagros-Hindu Kush-Himalaya Geodynamic Evolution, Geodynamics Series, American Geophysical Union, Washington, DC, USA, vol. 3, pp. 5-32.

Berberian M. and King G.C.P.; 1981: *Towards a paleogeography and tectonic evolution of Iran*. Can. J. Earth Sci., **18**, 210-265.

Bonham-Carter G.F.; 1995: *Geographic information systems for geoscientists: modelling with GIS, vol. 13, 1st ed*. Comput. Meth. Geosci., Elsevier Science, Amsterdam, The Netherland, 416 pp.

Carranza E.J.M.; 2008: *Geochemical anomaly and mineral prospectivity mapping in GIS, Vol. 11, 1st ed*. Handb. Explor. Environ. Geochem., Elsevier Science, Amsterdam, the Netherland, 368 pp.

Carranza E.J.M. and Hale M.; 2001: *Geologically constrained fuzzy mapping of gold mineralization potential, Baguio District, Philippines*. Nat. Resour. Res., **10**, 125-136, doi: 10.1023/A:1011500826411.

Cheng Q., Agterberg F.P. and Ballantyne S.B.; 1994: *The separation of geochemical anomalies from background by fractal methods*. J. Geochem. Explor., **51**, 109-130.

Clark D.A.; 1999: *Magnetic petrology of igneous intrusions-implications for exploration and magnetic interpretation*. Explor. Geophys., **20**, 5-26.

D'Ercole C., Groves D.I. and Knox-Robinson C.M.; 2000: *Using fuzzy logic within a geographic information system environment to enhance conceptually based prospectivity analysis of Mississippi Valley-type mineralisation*. Aust. J. Earth Sci., **47**, 913-927.

Davis J.C.; 2002: *Statistics and data analysis in geology, 3rd ed*. John Wiley and Sons Inc., New York, NY, USA, 656 pp.

Dehghan Nayeri R.; 2018: *Porphyry copper potential mapping in Narbaghi through TOPSIS multi-criteria decision making method*. MSc. Thesis, University of Tehran, Iran (in Persian).

Ghalamghash J.; 1998: *Geological map of Saveh 1:100000 survey sheet*. Geological Survey of Iran, Tehran, Iran.

Gokay M.K.; 1998: *Fuzzy logic usage in rock mass classifications*. J. Chamb. Min. Eng. Turk., **37**, 3-11, (in Turkish).

Imamalipour A. and Barak S.; 2019: *Geochemistry and tectonic setting of the volcanic host rocks of VMS mineralisation in the Qezil Dash area, NW Iran: implications for prospecting of Cyprus-type VMS deposits in the Khoy ophiolite*. Geol. Q., **63**, 435-473.

John D.A., Ayuso R.A., Barton M.D., Blakely R.J., Bodnar R.J., Dilles J.H., Gray F., Graybeal F.T., Mars J.C., McPhee D.K., Seal R.R., Taylor R.D. and Vikre P.G.; 2010: *Porphyry copper deposit model*. In: Mineral deposit models for resource assessment, U.S. Geological Survey, Scientific Investigations, Reston, VA, USA, Report 2010-5070-B, Chapter B, 169 pp.

Joly A., Porwal A. and McCuaig T.C.; 2012: *Exploration targeting for orogenic gold deposits in the Granites-Tanami Orogen: mineral system analysis, targeting model and prospectivity analysis*. Ore Geol. Rev., **48**, 349-383.

Kazemi K., Kananian A., Xiao Y. and Sarjoughian F.; 2018: *Chemical composition of rock-forming minerals and crystallization physicochemical conditions of the Middle Eocene I-type Haji Abad pluton, SW Buin-Zahra, Iran*. Arabian J. Geosci., **11**, 717, doi: 10.1007/s12517-018-4083-4

Klir G.J. and Yuan B.; 1995: *Fuzzy sets and fuzzy logic: theory and applications, vol 4*. Prentice Hall, Upper Saddle River, NJ, USA, 574 pp.

Knox-Robinson C.M.; 2000: *Vectorial fuzzy logic: a novel technique for enhanced mineral prospectivity mapping with reference to the orogenic gold mineralization potential of the Kalgoorlie Terrane, western Australia*. Aust. J. Earth Sci., **47**, 929-942.

Lee S.; 2007: *Application and verification of fuzzy algebraic operators to landslide susceptibility mapping*. Environ. Geol., **52**, 615-623.

Lindsay M.D., Betts P.G. and Ailleres L.; 2014: *Data fusion and porphyry copper prospectivity models, southeastern Arizona*. Ore Geol. Rev., **61**, 120-140.

Lisitsin V.A., González-Álvarez I. and Porwal A.; 2013: *Regional prospectivity analysis for hydrothermal-remobilised nickel mineral systems in western Victoria, Australia*. Ore Geol. Rev., **52**, 100-112.

Luo X. and Dimitrakopoulos R.; 2003: *Data-driven fuzzy analysis in quantitative mineral resource assessment*. Comput. Geosci., **29**, 3-13.

Mamdani E.H. and Assilian S.; 1975: *An experiment in linguistic synthesis with a fuzzy logic controller*. Int. J. Man-Mach. Stud., **7**, 1-13.

Masters T.; 1993: *Practical neural network recipes in C++, 1st ed*. Morgan Kaufmann Publishers, San Francisco, CA, USA, 493 pp.

Mizumoto M. and Tanaka K.; 1981: *Fuzzy sets and their operations*. Inf. Control, **48**, 30-48.

Monjezi M., Rezaei M. and Varjani A.Y.; 2009: *Prediction of rock fragmentation due to blasting in Gol-E-Gohar iron mine using fuzzy logic*. Int. J. Rock Mech. Min. Sci., **46**, 1273-1280.

Nguyen V.U. and Ashworth E.; 1985: *Rock mass classification by fuzzy sets*. In: Proc. 26th US Symposium on Rock Mechanics, Rapid City, SD, USA, pp. 937-945.

Nouri F., Azizi H., Stern R.J., Asahara Y., Khodaparast S., Madanipour S. and Yamamoto K.; 2018: *Zircon U-Pb dating, geochemistry and evolution of the Late Eocene Saveh magmatic complex, central Iran: partial melts of sub-continental lithospheric mantle and magmatic differentiation*. Lithos, **314-315**, 274-292.

Nykänen V., Groves D.I., Ojala V.J., Eilu P. and Gardoll S.J.; 2008: *Reconnaissance-scale conceptual fuzzy-logic prospectivity modelling for iron oxide copper-gold deposits in the northern Fennoscandian Shield, Finland*. Aust. J. Earth Sci., **55**, 25-38.

Osna T., Sezer E.A. and Akgun A.; 2014: *GeoFIS: an integrated tool for the assessment of landslide susceptibility*. Comput. Geosci., **66**, 20-30.

Porwal A., Carranza E.J.M. and Hale M.; 2003: *Knowledge-driven and data-driven fuzzy models for predictive mineral potential mapping*. Nat. Resour. Res., **12**, 1-25.

Porwal A., Das R.D., Chaudhary B., Gonzalez-Alvarez I. and Kreuzer O.; 2015: *Fuzzy inference systems for prospectivity modeling of mineral systems and a case-study for prospectivity mapping of surficial Uranium in Yeelirrie area, western Australia*. Ore Geol. Rev., **71**, 839-852.

Ramazi H. and Jalali M.; 2015: *Contribution of geophysical inversion theory and geostatistical simulation to determine geoelectrical anomalies*. Stud. Geophys. Geod., **59**, 97-112.

Rezaei M., Majdi A. and Monjezi M.; 2014: *An intelligent approach to predict unconfined compressive strength of rock surrounding access tunnels in longwall coal mining*. Neural Comput. Appl., **24**, 233-241.

Rezaei M., Asadizadeh M., Majdi A. and Hossaini M.F.; 2015: *Prediction of representative deformation modulus of longwall panel roof rock strata using Mamdani fuzzy system*. Int. J. Min. Sci. Technol., **25**, 23-30.

Sabri N., Aljunid S.A., Salim M.S., Badlishah R.B., Kamaruddin R. and Malek M.A.; 2013: *Fuzzy inference system: short review and design*. Int. Rev. Autom. Control, **6**, 441-449.

Shahabpour J.; 2005: *Tectonic evolution of the orogenic belt in the region located between Kerman and Neyriz*. J. Asian Earth Sci., **24**, 405-417.

Shams S., Monjezi M., Majd V.J. and Armaghani D.J.; 2015: *Application of fuzzy inference system for prediction of rock fragmentation induced by blasting*. Arabian J. Geosci., **8**, 10819-10832.

Sillitoe R.H.; 2010: *Porphyry copper systems*. Econ. Geol., **105**, 3-41, doi: 10.2113/gsecongeo.105.1.3.

Singer D.A., Berger V.I. and Moring B.C.; 2002: *Porphyry copper deposits of the world: database, maps, and preliminary analysis*. U.S. Geological Survey, Reston, VA, USA, Open-File Report 2002-268, 61 pp., doi: 10.3133/ofr02268.

Stöcklin J.; 1968: *Structural history and tectonics of Iran: a review*. Am. Assoc. Pet. Geol. Bull., **52**, 1229-1258.

Tang X.; 2004: *Spatial object modeling in fuzzy topologicals spaces: with applications to land cover change*. PhD Thesis, International Institute for Geo-Information Science and Earth Observation, Enschede, the Netherland, 241 pp.

Tangestani M.H. and Moore F.; 2003: *Mapping porphyry copper potential with a fuzzy model, northern Shahr-eBabak, Iran*. Aust. J. Earth Sci., **50**, 311-317.

Thoman M.W., Zonge K.L. and Liu D.; 1998: *Geophysical case history of North Silver Bell, Pima County, Arizona: a supergene-enriched porphyry copper deposit*. In: Selected Papers, Ellis R.B., Irvine R. and Fritz F. (eds), Practical Geophysics Short Course, Northwest Mining Association, Spokane, WA, USA, paper 4, 42 pp.

Turcotte D.L.; 1997: *Fractal and chaos in geology and geophysics, 2nd ed*. Cambridge University Press, Cambridge, UK, 398 pp., doi: 10.1017/CBO9781139174695.

Zadeh L.A.; 1965: *Fuzzy sets*. Inf. Control, **8**, 338-353.

Corresponding author: Maysam Abedi
Geo-Exploration Targeting Lab (GET-Lab), School of Mining Engineering,
College of Engineering, University of Tehran
North Kargar street, Tehran, Iran
Phone: +98 0216 1114563; e-mail: MaysamAbedi@ut.ac.ir